# Electronic Supplementary Information

## Electrochemically fabricated $MoO_3$-$MoO_2$@NiMo heterostructure catalyst with Pt-like activity for pH-universal hydrogen evolution reaction

Juhae Park[a], Hyunki Kim[a], Gyeong Ho Han[a], Junhyeong Kim[a], Sung Jong Yoo[b], Hyoung-Juhn Kim[b], Sang Hyun Ahn[a,*]

[a]*School of Chemical Engineering and Material Science, Chung-Ang University, Seoul 06974, Republic of Korea*

[b]*Center for Hydrogen Fuel Cell Research, Korea Institute of Science and Technology (KIST), Seoul 02792, Republic of Korea*

Corresponding author

*E-mail: shahn@cau.ac.kr (Sang Hyun Ahn)

**Table S1** Summary on HER performance of Ni or Mo-containing non-noble metal-based catalysts in acidic electrolyte from recent literature.

| Catalysts | Electrolyte | Overpotential @ −10 mA cm$^{-2}$ / mV | Tafel slope / mV dec$^{-1}$ | Loading amount / mg cm$^{-2}$ | Reference |
|---|---|---|---|---|---|
| E-NiMo-7.5@0.02 | 0.5 M $H_2SO_4$ | 27.9 | 25.3 | 0.88 | This work |
| MoNiS@NiS/CC | 0.5 M $H_2SO_4$ | 33 | 80 | | 1 |
| $Ni_{43}Ru_{57}$ | 0.5 M $H_2SO_4$ | 41 | 31 | 0.28 | 2 |
| 1Ni-0.5$Mo_2C$/GNS | 0.5 M $H_2SO_4$ | 49.6 | 54.7 | 0.38 | 3 |
| NiRu@N-C | 0.5 M $H_2SO_4$ | 50 | 36 | | 4 |
| $Ni_{0.89}Co_{0.11}Se_2$ | 0.5 M $H_2SO_4$ | 52 | 39 | 2.16 | 5 |
| rGO-$MoO_{3-x}$–MoRu(28) | 0.5 M $H_2SO_4$ | 60 | 40 | | 6 |
| CoP-$MoO_2$/MF | 0.5 M $H_2SO_4$ | 65 | 85 | 4.17 | 7 |
| 3D $Mo_2C$@$MoS_2$ NS | 0.5 M $H_2SO_4$ | 67 | 37 | | 8 |
| Mo–$Ni_2P$ NWs/NF | 0.5 M $H_2SO_4$ | 67 | 77 | 1.13 | 9 |
| $MoSe_2$-NiSe@carbon(MN11) | 0.5 M $H_2SO_4$ | 67 | 76.3 | 0.28 | 10 |
| $Ni_2P$/OMM-CoN-C | 0.5 M $H_2SO_4$ | 68 | 37 | 0.26 | 11 |
| 3D $Ni_2P$ NPs | 0.5 M $H_2SO_4$ | 69 | 55 | 10.8 | 12 |
| Ni-$Mo_2C$@C | 0.5 M $H_2SO_4$ | 72 | 65.8 | 0.531 | 13 |
| Ni-doped FeP/C | 0.5 M $H_2SO_4$ | 72 | 54 | 0.4 | 14 |
| MoP/CNT | 0.5 M $H_2SO_4$ | 83 | 60 | 0.5 | 15 |
| $MoO_2$/$MoS_2$\|P | 0.5 M $H_2SO_4$ | 85 | 19.7 | | 16 |
| MoP@C | 0.5 M $H_2SO_4$ | 88 | 50.4 | | 17 |
| $MoSe_2$ NS/$MoO_2$ NB/CNT-M | 0.5 M $H_2SO_4$ | 97 | 69.7 | | 18 |
| $Mo_2C$/CTSS | 0.5 M $H_2SO_4$ | 97 | 48 | 0.75 | 19 |

**Table S2** Summary on HER performance of Ni or Mo-containing non-noble metal-based catalysts in neutral electrolyte from recent literature.

| **Catalysts** | **Electrolyte** | **Overpotential @ −10 mA cm$^{-2}$ / mV** | **Tafel slope / mV dec$^{-1}$** | **Loading amount / mg cm$^{-2}$** | **Reference** |
|---|---|---|---|---|---|
| E-NiMo-7.5@0.02 | 1.0 M PBS | 82.6 | 188.4 | 0.88 | This work |
| Ni-$B_{0.54}$ | 1.0 M PBS | 54 | 77 | 1.40 | 20 |
| $NiCo_2P_x$/CF | 1.0 M PBS | 63 | 63.3 | | 21 |
| N−Ni | 1.0 M PBS | 64 | 106 | | 22 |
| Mo–$Ni_2P$ NWs/NF | 1.0 M PBS | 84 | 85 | 1.13 | 9 |
| $Ni_{0.89}Co_{0.11}Se_2$ | 1.0 M PBS | 82 | 78 | 2.16 | 5 |
| $(Fe_{0.048}Ni_{0.952})_2P$ | 1.0 M PBS | 90 | 82.7 | 1.0 | 23 |
| MoP/CNT | 1.0 M PBS | 102 | 115 | 0.5 | 15 |
| Ni–Co–Fe–P/NF-3-75 | 1.0 M PBS | 104 | 121.7 | | 24 |
| $Ni_xP$/CNT | 1.0 M PBS | 105 | 100 | 10.0 | 25 |
| Ni-doped FeP/C | 1.0 M PBS | 117 | 70 | 0.4 | 14 |
| NiWS/CF | 0.2 M PBS | 120 | 244 | | 26 |
| 3D $Mo_2C$@$MoS_2$ NS | 1.0 M PBS | 121 | 46 | | 8 |
| MoP/NPG | 1.0 M PBS | 150 | 102 | 0.28 | 27 |
| $Co_2Ni_1N$ | 1.0 M PBS | 152.8 | 90.3 | 0.24 | 28 |
| 1T′$MoS_2/Ni_{2+\delta}O_\delta(OH)_{2-\delta}$ (1:1) | 1.0 M PBS | 153 | 106 | 0.8 | 29 |
| Co-30Ni–B | 0.5 M KPi | 170 | 51 | 2.1 | 30 |
| NCP holey nanosheet | 1 M PBS | 170 | 106 | | 31 |
| $CoMoS_4$ NS/CC | 1.0 M PBS | 183 | 116 | 1.48 | 32 |
| MoP@NC | 1.0 M PBS | 191 | 95 | 0.28 | 33 |

**Table S3** Summary on HER performance of Ni or Mo-containing non-noble metal-based catalysts in alkaline electrolyte from recent literature.

| Catalysts | Electrolyte | Overpotential @ −10 mA cm$^{-2}$ / mV | Tafel slope / mV dec$^{-1}$ | Loading amount / mg cm$^{-2}$ | Reference |
|---|---|---|---|---|---|
| E-NiMo-7.5@0.02 | 1.0 M KOH | 33.4 | 96.8 | 0.88 | This work |
| $MoNi_4/MoO_2$@Ni | 1.0 M KOH | 15 | 30 | 43.4 | 34 |
| NiMo-NWs/Ni-foam | 1.0 M KOH | 30 | 86 | 0.41 | 35 |
| NiRu@N–C | 1.0 M KOH | 32 | 64 | | 4 |
| $Ni(OH)_2$–$NiMoO_x$/NF | 1.0 M KOH | 36 | 38 | | 36 |
| NMOU400 | 1.0 M KOH | 40 | 116 | | 37 |
| CoP–$MoO_2$/MF | 1.0 M KOH | 42 | 127 | 4.17 | 7 |
| MoP@$Ni_3P$/NF | 1.0 M KOH | 45 | 56 | | 38 |
| $MoO_2/MoS_2$\|P | 1.0 M KOH | 45 | 64.2 | | 16 |
| MoP@C | 1.0 M KOH | 49 | 54 | | 17 |
| Flame-like Ni(OH)2/NF | 1.0 M KOH | 56.4 | 52.8 | 0.71 | 39 |
| R□$MoS_2$@NF | 1.0 M KOH | 71 | 100 | 0.4-0.5 | 40 |
| NiMo-EDA | 1.0 M KOH | 72 | 89 | 0.35 | 41 |
| 3D $Ni_2P$ NPs | 1.0 M KOH | 73 | 73 | 10.8 | 12 |
| NiMo/NF | 1.0 M KOH | 73 | 37.2 | 0.88 | 42 |
| Mo–$Ni_2P$ NWs/NF | 1.0 M KOH | 78 | 109 | 1.13 | 9 |
| $Ni(OH)_2/MoS_2$ | 1.0 M KOH | 80 | 60 | 4.8 | 43 |
| $Ni_{0.89}Co_{0.11}Se_2$ | 1.0 M KOH | 85 | 52 | 2.16 | 5 |
| MoP/CNT | 1.0 M KOH | 86 | 73 | | 15 |
| 3D $Mo_2C$@$MoS_2$ NS | 1.0 M KOH | 86 | 39 | | 8 |

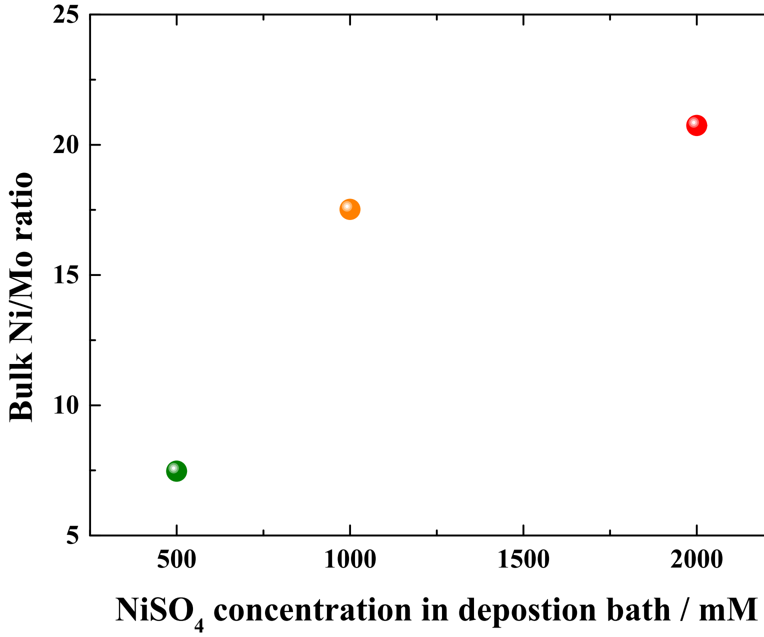


**Fig. S1** Bulk Ni/Mo ratio according to $NiSO_4$ concentration in deposition bath.

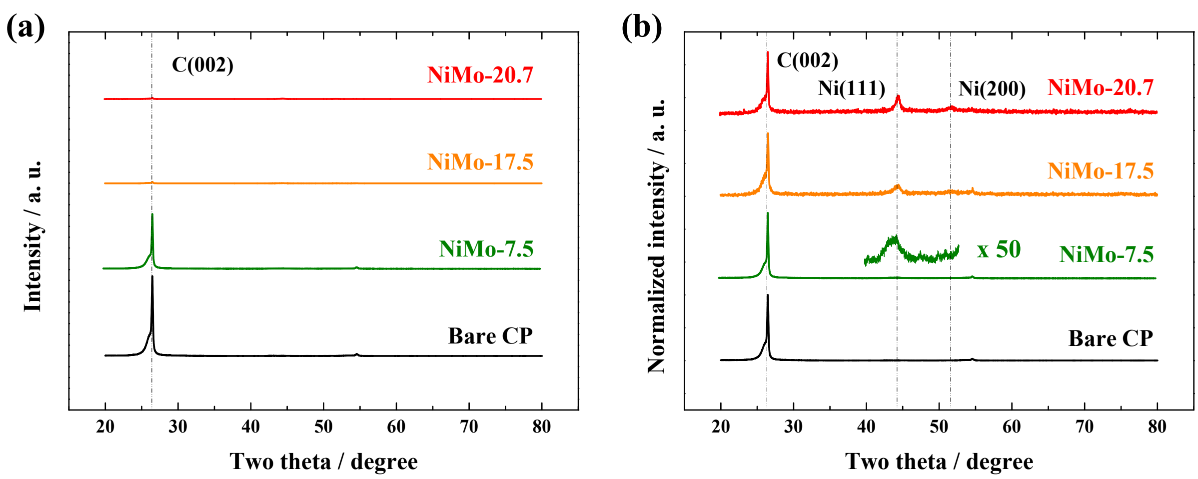


**Fig. S2** (a) XRD patterns of CP substrate and NiMo-#. (b) The XRD patterns with normalized intensity by C(002) peak.

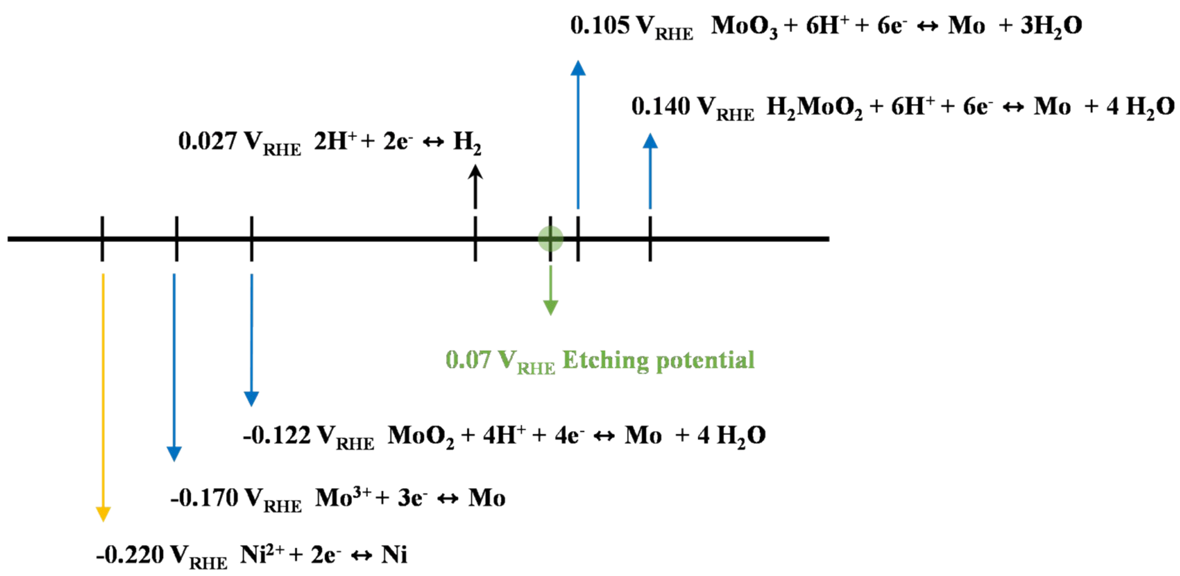


**Fig. S3** Scale of various applied potentials and potentials of electrochemical reactions.

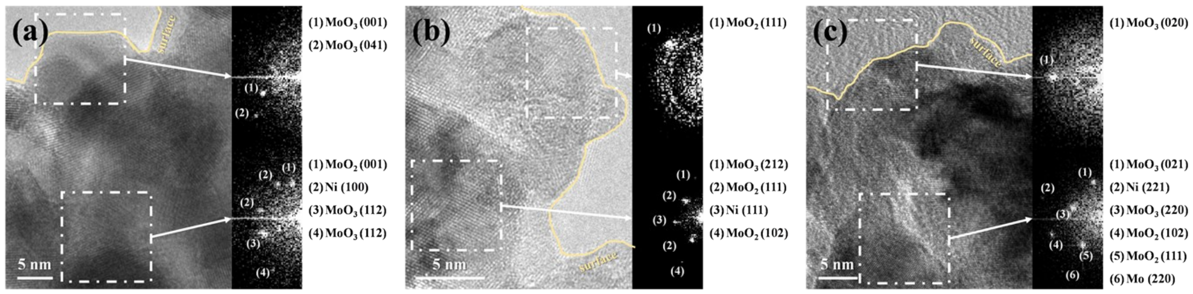


**Fig. S4** HRTEM images of (a) E-NiMo-7.5, (b) E-NiMo-17.5, and (c) E-NiMo-20.7 with FFT patterns.

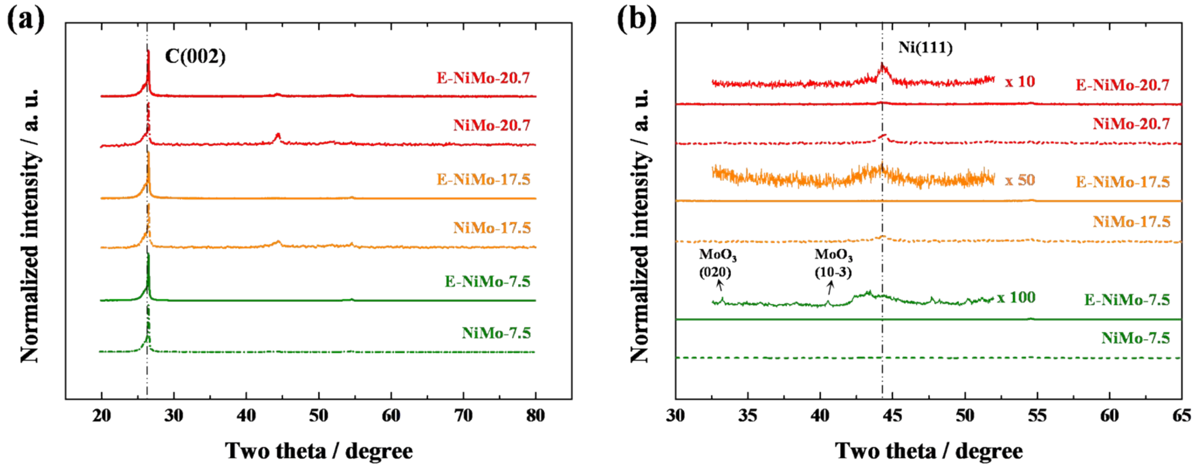


**Fig. S5** (a) XRD patterns of NiMo-# and E-NiMo-# with normalized intensity by C(002) peak.

(b) Expanded XRD patterns of (a).

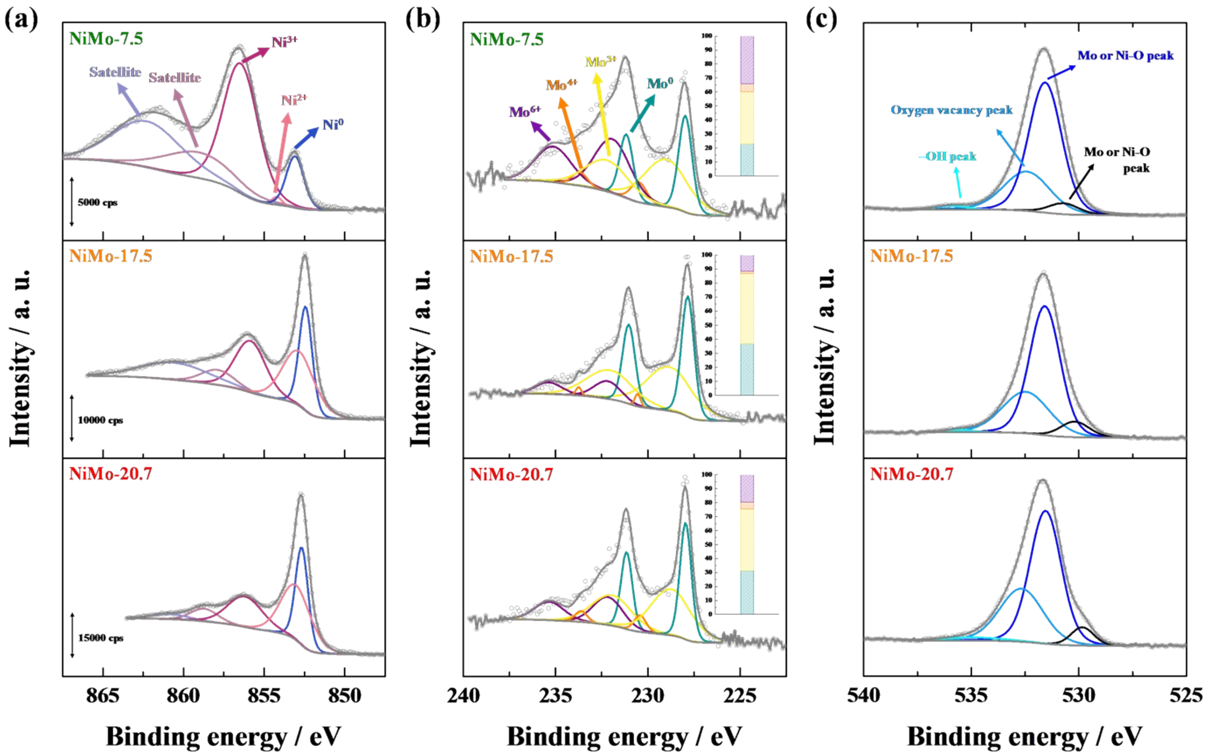


**Fig. S6** (a) Ni 2p , (b) Mo 3d, and (c) O 1s XPS spectra for NiMo-# samples.

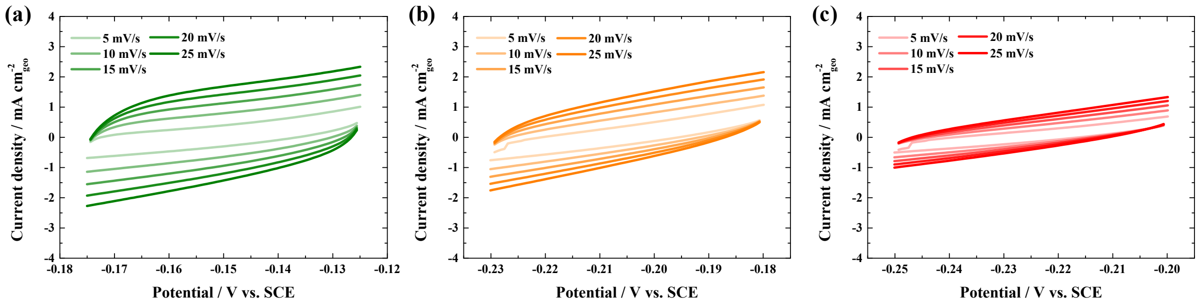


**Fig. S7** Repeated CV curves of (a) E-NiMo-7.5, (b) E-NiMo-17.5, and (c) E-NiMo-20.7 at various scan rates in $N_2$-purged 0.5 M $H_2SO_4$ electrolyte.

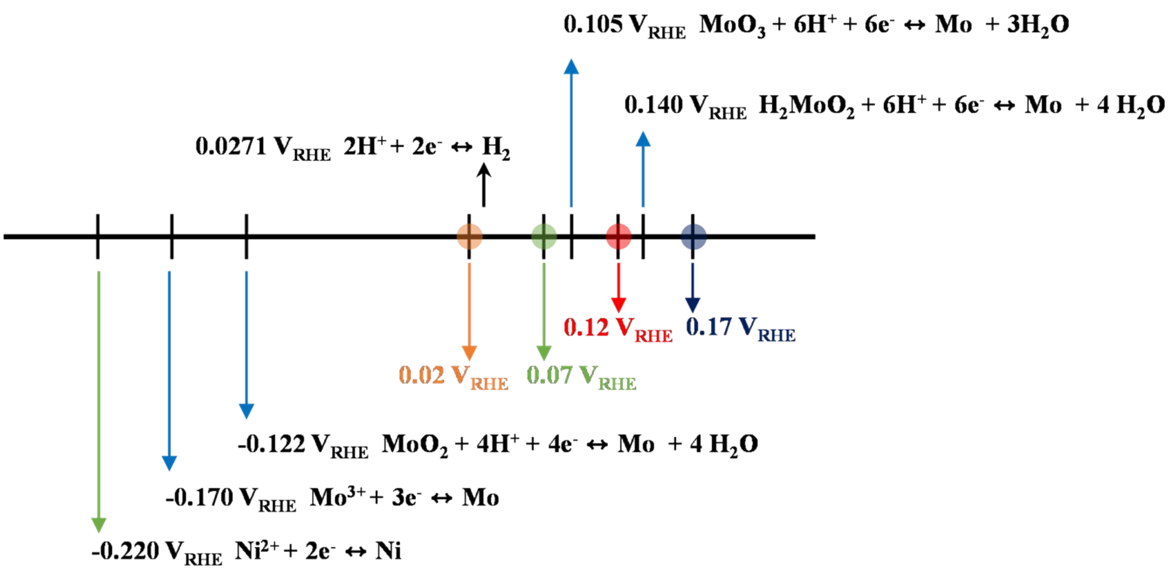


**Fig. S8** Scale of various applied potentials and potentials of electrochemical reactions.

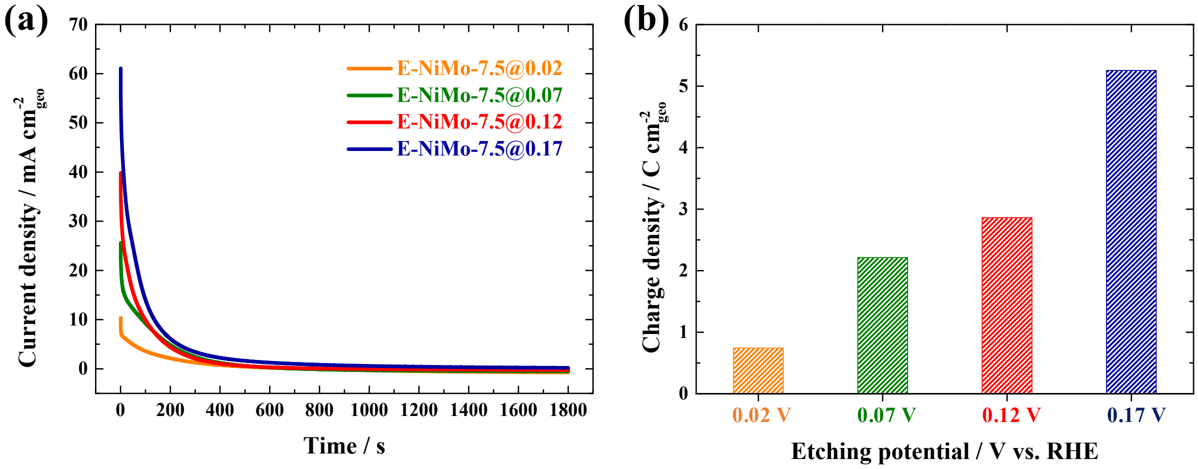


**Fig. S9** (a) Chronoamperometry of E-NiMo-7.5@# at various potentials for 1800 s. (b) Calculated anodic charge densities.

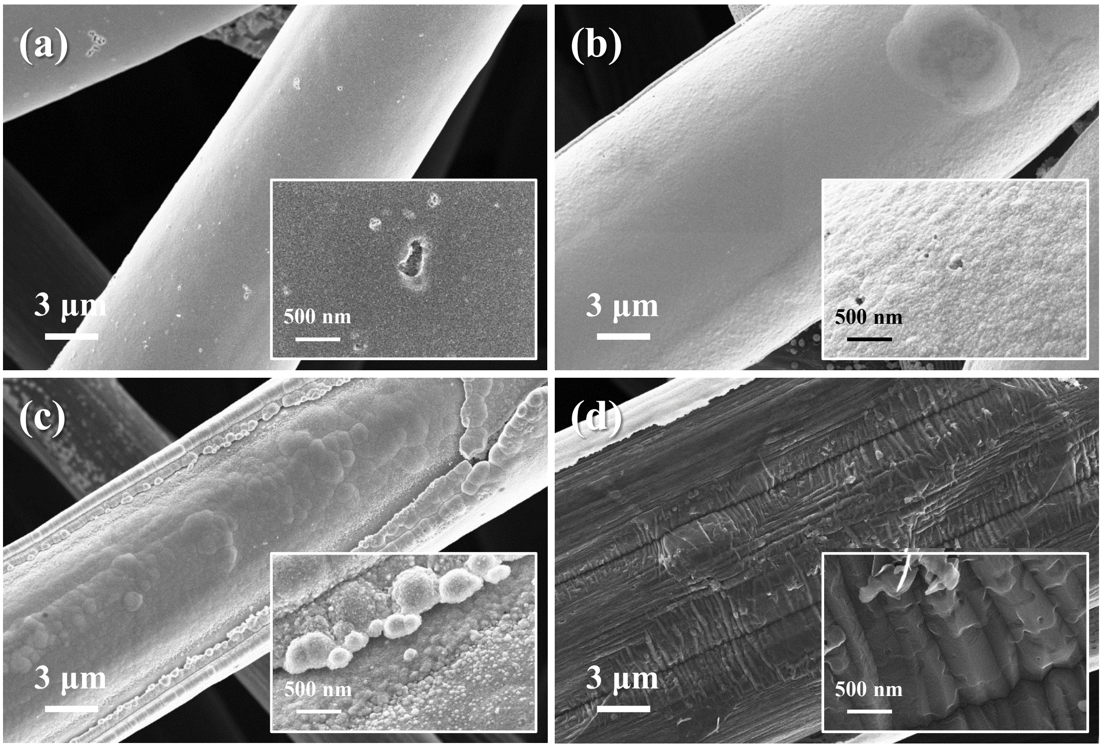


**Fig. S10** FESEM images of (a) E-NiMo-7.5@0.02, (b) E-NiMo-7.5@0.07, (c) E-NiMo-7.5@0.12, and (d) E-NiMo-7.5@0.17.

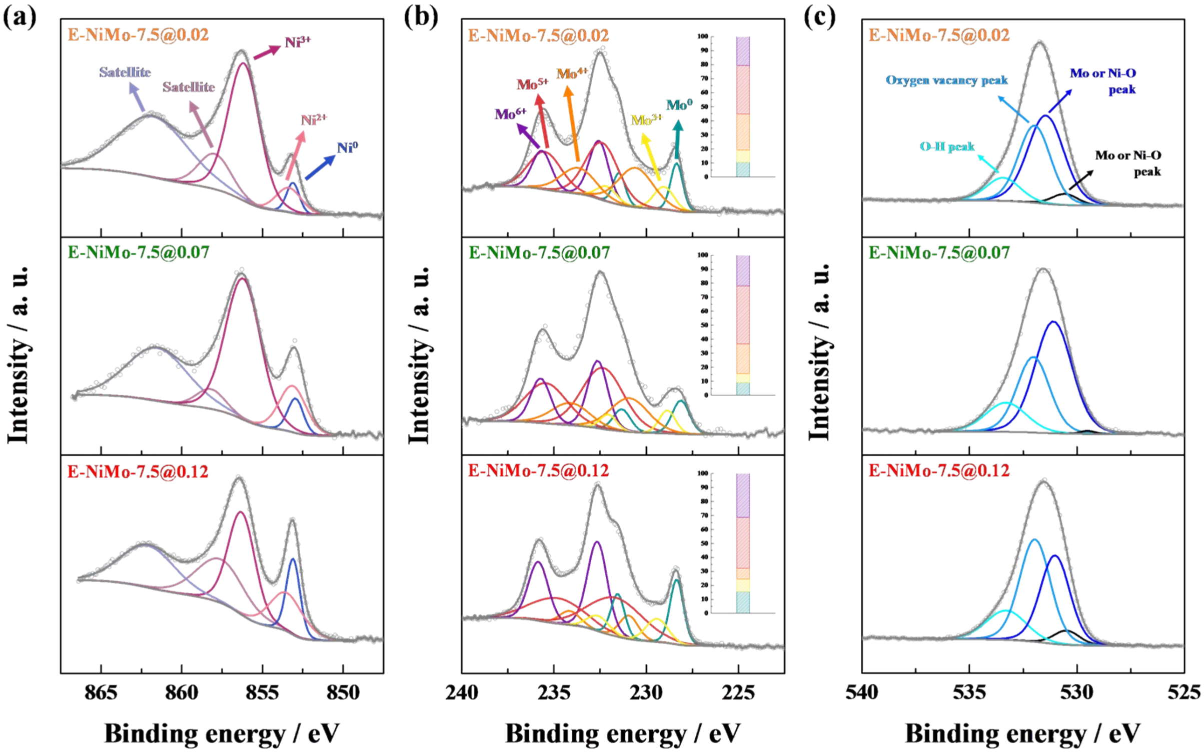


**Fig. S11** (a) Ni 2p , (b) Mo 3d, and (c) O 1s XPS spectra for E-NiMo-7.5@# samples.

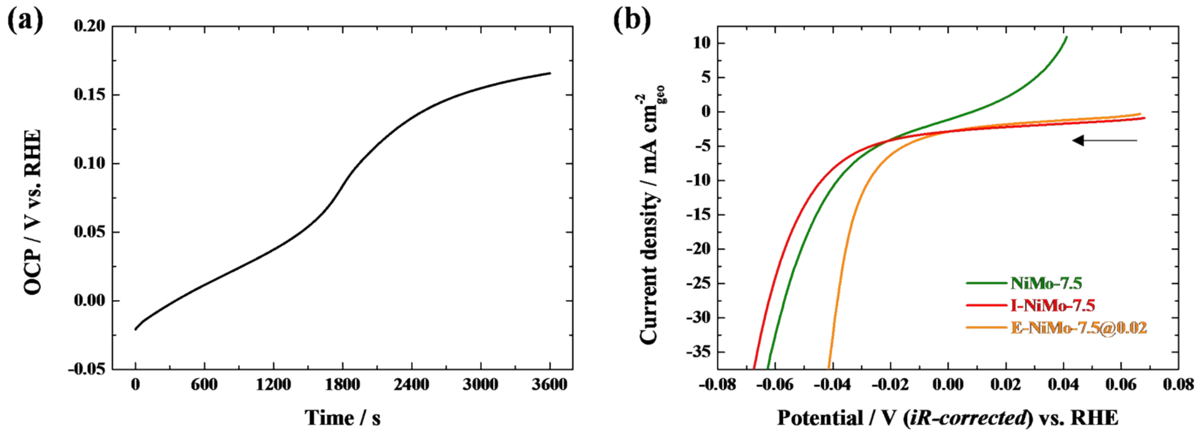


**Fig. S12** (a) OCP of NiMo-7.5 in 0.5 M $H_2SO_4$ electrolyte as a function of time. (b) LSV of NiMo-7.5, E-NiMo-7.5@0.02, and I-NiMo-7.5 at a scan rate of 5 mV/s in in 0.5 M $H_2SO_4$ electrolyte.

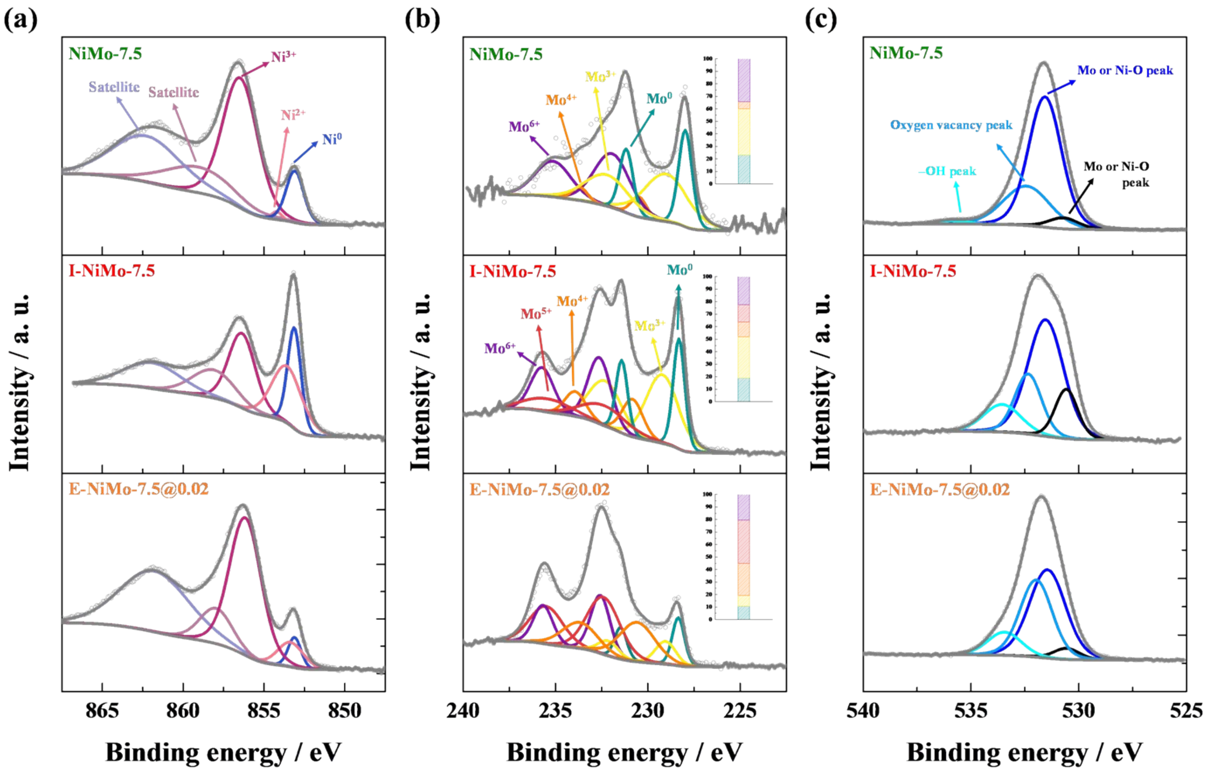


**Fig. S13** XPS survey spectra for NiMo-7.5, I-NiMo-7.5, and E-NiMo-7.5@0.02.

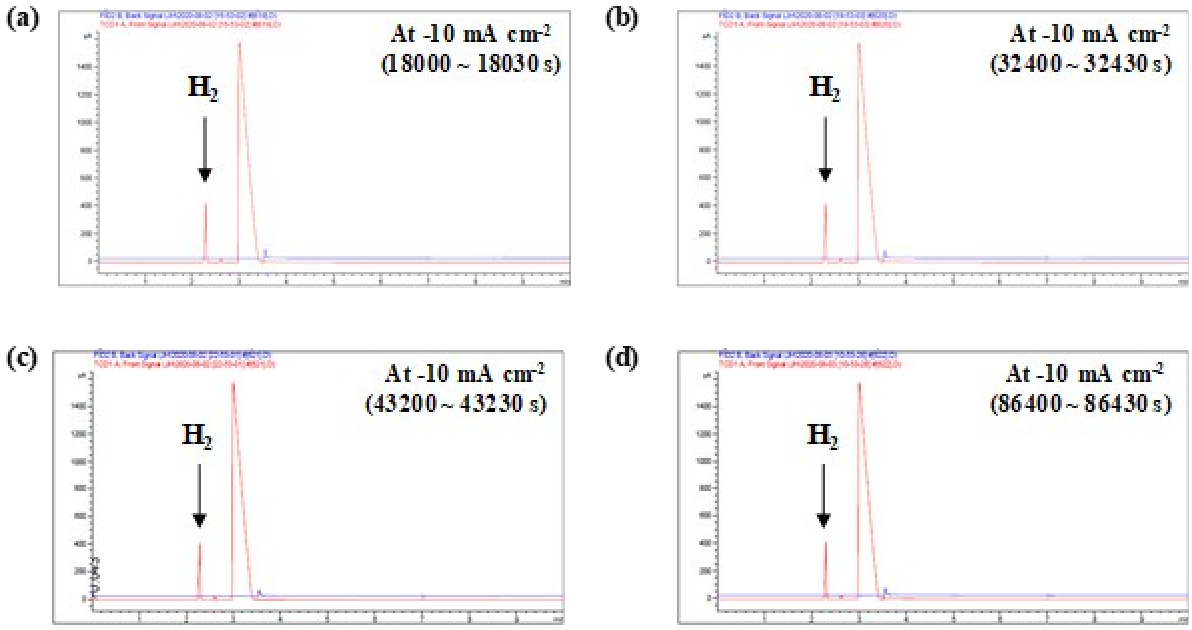


**Fig. S14** Gas chromatography analysis of E-NiMo-7.5@0.02 depending on the measuring time.

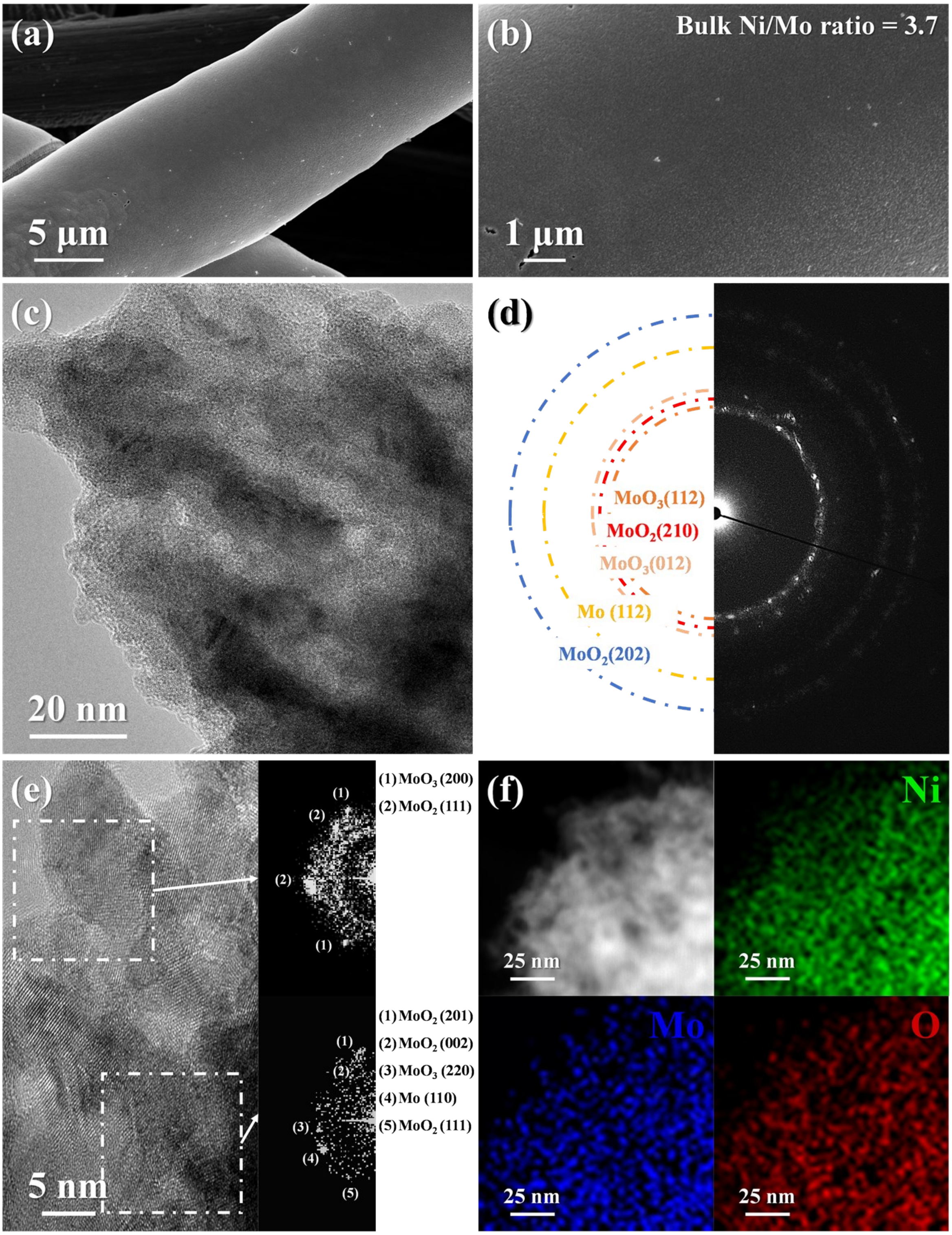


**Fig. S15** E-NiMo-7.5@0.02 after stability test. FESEM images at (a) low and (b) high magnification. (c) HRTEM image. (d) SAED pattern of (c). (e) HRTEM image with FFT patterns. (f) Dark field image and elemental mapping for Ni, Mo, and O.

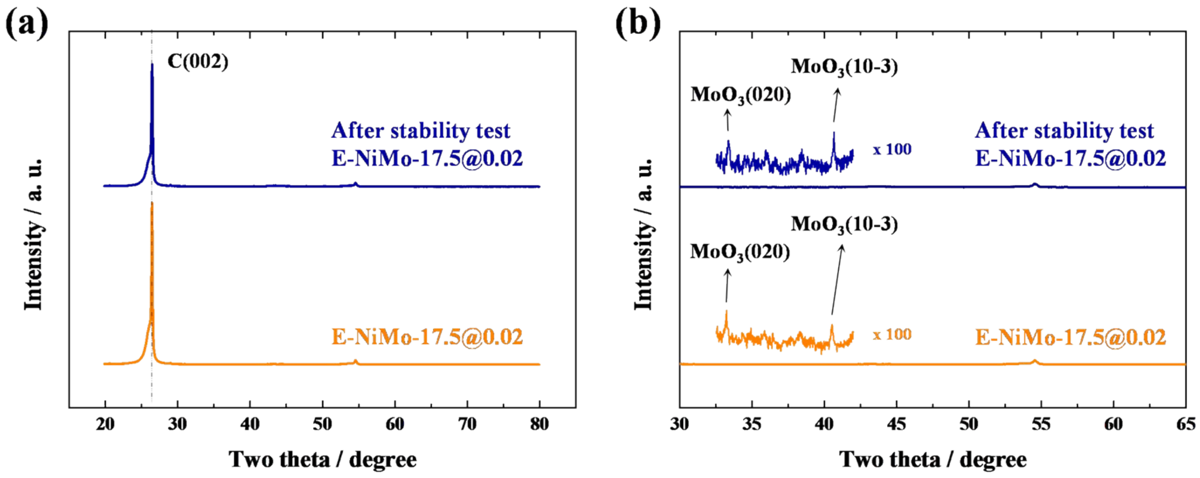


**Fig. S16** (a) XRD patterns of E-NiMo-7.5@0.02 before and after stability test (b) Expanded XRD patterns of (a).

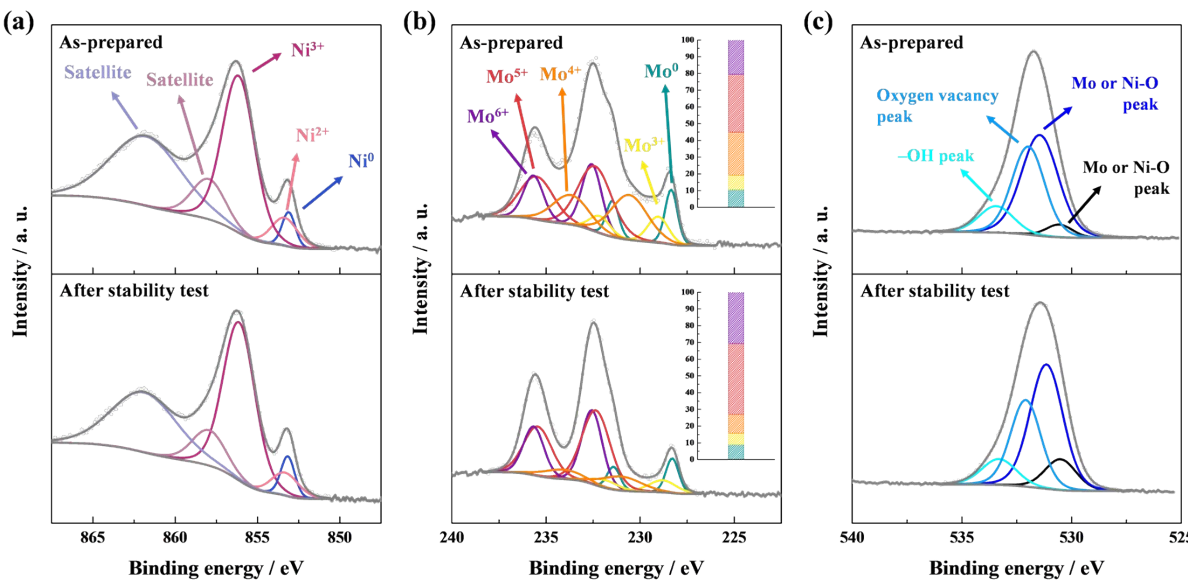


**Fig. S17.** (a) Ni 2p, (b) Mo 3d, and (c) O 1s XPS spectra for E-NiMo-7.5@0.02 samples before and after stability test.

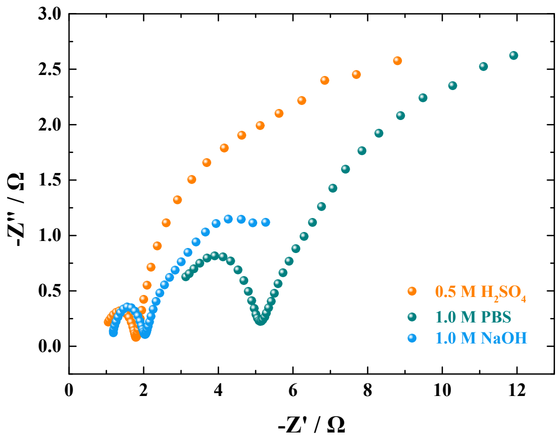


**Fig. S18.** Nyquist plots of E-NiMo-7.5@0.02 measured at −10 mA/cm$^2$ in $N_2$-purged 0.5 M $H_2SO_4$, 1.0 M PBS, and 1.0 M NaOH electrolytes.

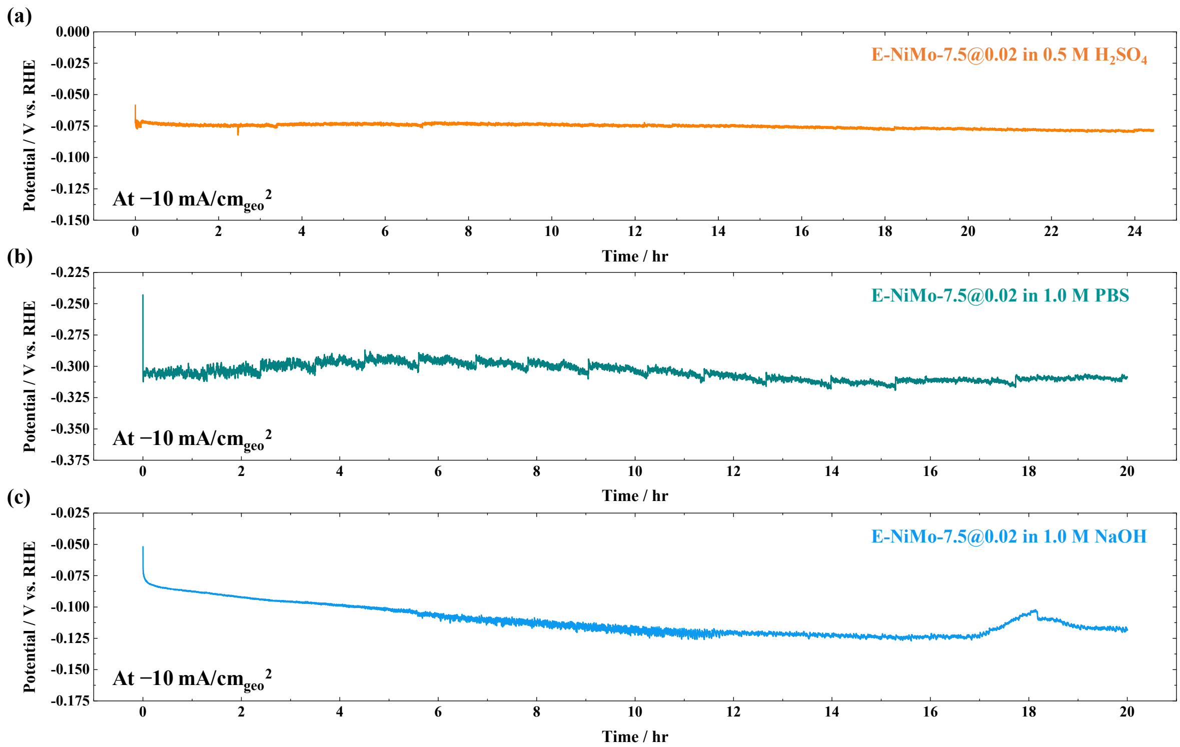


**Fig. S19** Chronopotentiometry at constant current density of −10 mA/cm$^2$ for 24 h in $N_2$-purged (a)0.5 M $H_2SO_4$ for 20 hr in $N_2$-purged (b)1.0 M PBS and (c)1.0 M NaOH electrolytes in an H-type cell.

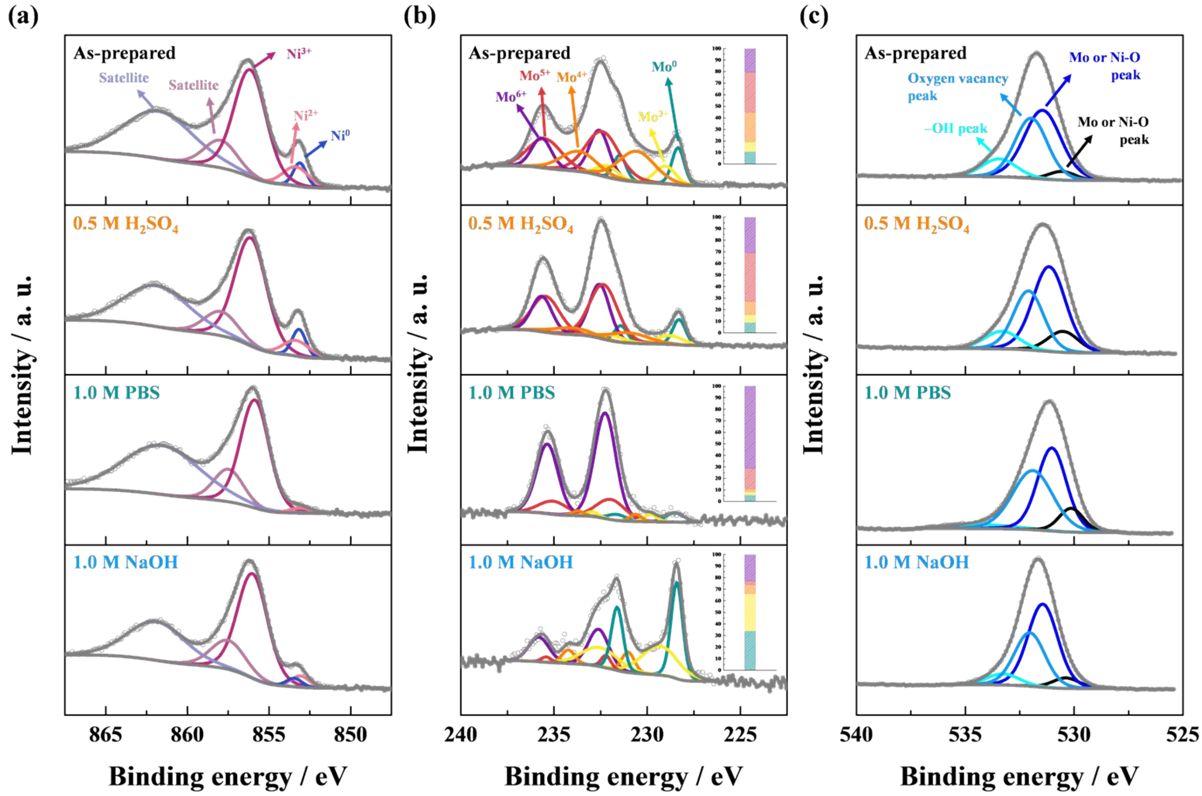


**Fig. S20.** Ni 2p, Mo 3d, and O 1s spectra of (a) as-prepared E-NiMo-7.5@0.02 and after the long-term stability at −10 mA/cm$^2$ in $N_2$-purged (b) 0.5 M $H_2SO_4$, (c) 1.0 M PBS, and (d) 1.0 M NaOH electrolytes.

**References**

[1] Y. Xie, Y. Liu, Z. Yang, Interfaces engineering of MoNi-based sulfides electrocatalysts for hydrogen evolution reaction in both acid and alkaline media, Int. J. Hydrog. Energy 45 (2020) 6500–6507.

[2] C. Zhang, Y. Liu, Y. Chang, Y. Lu, S. Zhao, D. Xu, Z. Dai, M. Han, J. Bao, Component-controlled synthesis of necklace-like hollow $Ni_XRu_y$ nanoalloys as electrocatalysts for hydrogen evolution reaction, ACS Appl. Mater. Interfaces 9 (2017) 17326–17336.

[3] Y. Zhou, T. Lin, X. Luo, Z. Yan, J. Wu, J. Wang, Y. Shen, Mechanistic study on nickel-molybdenum based electrocatalysts for the hydrogen evolution reaction, J. Catal. 388 (2020) 122–129.

[4] Y. Xu, S. Yin, C. Li, K. Deng, H. Xue, X. Li, H. Wang, L. Wang, Low-ruthenium-content NiRu nanoalloys encapsulated in nitrogen-doped carbon as highly efficient and pH-universal electrocatalysts for the hydrogen evolution reaction, J. Mater. Chem. A 6 (2018) 1376–1381.

[5] B. Liu, Y.-.F. Zhao, H.-Q. Peng, Z.-Y. Zhang, C.-K. Sit, M.-F. Yuen, T.-R. Zhang, C.-S. Lee, W.-J. Zhang, Nickel–cobalt diselenide 3D mesoporous nanosheet networks supported on Ni foam: An all-pH highly efficient integrated electrocatalyst for hydrogen evolution, Adv Mater. 29 (2019) 1606521.

[6] S. Liu, C. Chen, Y. Zhang, Q. Zheng, S. Zhang, X. Mu, C. Chen, J. Ma, S. Mu, Vacancy-coordinated hydrogen evolution reaction on $MoO_{3-x}$ anchored atomically dispersed MoRu pairs, J. Mater. Chem. A 7 (2019) 14466–14472.

[7] H. Zhao, Z. Li, X. Dai, M. Cui, F. Nie, X. Zhang, Z. Ren, Z. Yang, Y. Gan, X. Yin, Y. Wang, W. Song, Heterostructured $CoP/MoO_2$ on Mo foil as high-efficiency electrocatalysts for the hydrogen evolution reaction in both acidic and alkaline media, J. Mater. Chem. A 8 (2020) 6732–6739.

[8] S. Yang, Y. Wang, H. Zhang, Y. Zhang, L. Liu, L. Fang, X. Yang, X. Gu, Y. Wang, Unique three-dimensional $Mo_2C@MoS_2$ heterojunction nanostructure with S vacancies as outstanding all-pH range electrocatalyst for hydrogen evolution, J. Catal. 371 (2019) 20–26.
[9] Y. Sun, L. Hang, Q. Shen, T. Zhang, H. Li, X. Zhang, X. Lyu, Y. Li, Mo doped $Ni_2P$ nanowire arrays: an efficient electrocatalyst for the hydrogen evolution reaction with enhanced activity at all pH values, Nanoscale 9 (2017) 16674–16679.
[10] C. Liu, K. Wang, X. Zheng, X. Liu, Q. Liang, Z. Chen, Rational design of $MoSe_2$-NiSe@carbon heteronanostructures for efficient electrocatalytic hydrogen evolution in both acidic and alkaline media, Carbon 139 (2018) 1–9.
[11] T. Sun, J. Dong, Y. Huang, W. Ran, J. Chen, L. Xu, Highly active and stable electrocatalyst of $Ni_2P$ nanoparticles supported on 3D ordered macro-/mesoporous Co–N-doped carbon for acidic hydrogen evolution reaction, J. Mater. Chem. A 6 (2018) 12751–12758.
[12] Y. Lin, L. He, T. Chen, D. Zhou, L. Wu, X. Hou, C. Zheng, Cost-effective and environmentally friendly synthesis of 3D $Ni_2P$ from scrap nickel for highly efficient hydrogen evolution in both acidic and alkaline media, J. Mater. Chem. A 6 (2018) 4088–4094.
[13] F. Yu, Y. Gao, Z. Lang, Y. Ma, L. Yin, J. Du, H. Tan, Y. Wang, Y. Li, Electrocatalytic performance of ultrasmall $Mo_2C$ affected by different transition metal dopants in hydrogen evolution reaction, Nanoscale 10 (2018) 6080–6087.
[14] X. F. Lu, L. Yu, X. W. Lou, Highly crystalline Ni-doped FeP/carbon hollow nanorods as all-pH efficient and durable hydrogen evolving electrocatalysts, Sci. Adv. 5 (2019) eaav6009.
[15] X. Zhang, X. Yu, L. Zhang, F. Zhou, Y. Liang, R. Wang, Molybdenum phosphide/carbon nanotube hybrids as pH-universal electrocatalysts for hydrogen evolution reaction, Adv. Funct. Mater. 28 (2018) 1706523.

[16] C. Jian, W. Hong, Q. Cai, J. Li, W. Liu, Surface electron state engineering enhanced hydrogen evolution of hierarchical molybdenum disulfide in acidic and alkaline media, Appl. Catal. B-Environ. 266 (2020) 118649.

[17] G. Li, Y. Sun, J. Rao, J. Wu, A. Kumar, Q. N. Xu, C. Fu, E. Liu, G. R. Blake, P. Werner, B. Shao, K. Liu, S. Parkin, X. Liu, M. Fahlman, S.-C. Liou, G. Auffermann, J. Zhang, C. Felser, X. Feng, Carbon-tailored semimetal MoP as an efficient hydrogen evolution electrocatalyst in both alkaline and acid media, Adv. Energy Mater. 8 (2018) 1801258.

[18] L. J. Yang, Y. Q. Deng, X. F. Zhang, H. Liu, W. J. Zhou, $MoSe_2$ nanosheet/$MoO_2$ nanobelt/carbon nanotube membrane as flexible and multifunctional electrodes for full water splitting in acidic electrolyte, Nanoscale, 10 (2018) 9268–9275.

[19] Z. Xu, G. Zhang, C. Lu, H. Tian, X. Xi, R. Liu, D. Wu, Molybdenum carbide nanoparticle decorated hierarchical tubular carbon superstructures with vertical nanosheet arrays for efficient hydrogen evolution, J. Mater. Chem. A 6 (2018) 18833–18838.

[20] P. Zhang, M. Wang, Y. Yang, T. Yao, H. Han, L. Sun, Electroless plated Ni–$B_x$ films as highly active electrocatalysts for hydrogen production from water over a wide pH range, Nano Energy 19 (2016) 98–107.

[21] R. Zhang, X. Wang, S. Yu, T. Wen, X. Zhu, F. Yang, X. Sun, X. Wang, W. Hu, Ternary $NiCo_2P_x$ nanowires as pH-universal electrocatalysts for highly efficient hydrogen evolution reaction, Adv. Mater. 29 (2017) 1605502.

[22] B. You, X. Liu, G. Hu, S. Gul, J. Yano, D.-E. Jiang, Y. Sun, Universal surface engineering of transition metals for superior electrocatalytic hydrogen evolution in neutral water, J. Am. Chem. Soc. 139 (2017) 12283–12290.

[23] W. Zhang, Y. Zou, H. Liu, S. Chen, X. Wang, H. Zhang, X. She, D. Yang, Single-crystalline $(Fe_xNi_{1-x})_2P$ nanosheets with dominant {011¯1¯} facets: Efficient electrocatalysts for hydrogen evolution reaction at all pH values, Nano Energy 56 (2019) 813–822.

[24] K. Wang, Y. Si, Z. Lv, T. Yu, X. Liu, G. Wang, G. Xie, L. Jiang, Efficient and stable Ni–Co–Fe–P nanosheet arrays on Ni foam for alkaline and neutral hydrogen evolution, Int. J. Hydrog. Energy 45 (2020) 2504–2512.

[25] S. Wnag, L. Zhang, X. Li, R. Zhang, Y. Zhang, H. Zhu, Sponge-like nickel phosphide–carbon nanotube hybrid electrodes for efficient hydrogen evolution over a wide pH range, Nano Res. 2 (2017) 415–425.

[26] S.-S. Lu, X. Shang, L.-M. Zhang, B. Dong, W.-K. Gao, F.-N. Dai, B. Liu, Y.-M. Chai, C.-G. Liu, Heterostructured binary Ni-W sulfides nanosheets as pH-universal electrocatalyst for hydrogen evolution, Appl. Surf. Sci. 445 (2018) 445–453.

[27] R. Ge, J. Huo, T. Liao, Y. Liu, M. Zhu, Y. Li, J. Zhang, W. Li, Hierarchical molybdenum phosphide coupled with carbon as a whole pH-range electrocatalyst for hydrogen evolution reaction, Appl. Catal. B-Environ. 260 (2020) 118196.

[28] X. Feng, H. Wang, X. Bo, L. Guo, Bimetal–organic framework-derived porous rodlike cobalt/nickel nitride for all-pH value electrochemical hydrogen evolution, ACS Appl. Mater. Interfaces 11 (2019) 8018–8024.

[29] X. Zhang, Y. Liang, Nickel hydr(oxy)oxide nanoparticles on metallic $MoS_2$ nanosheets: A synergistic electrocatalyst for hydrogen evolution reaction, Adv. Sci. 5 (2018) 1700644.

[30] S. Gupta, N. Patel, R. Fernandes, A. Dashora, A. K. Yadav, D. Bhattacharyya, S. N. Jha, A. Miotello, D. C. Kothari, Co–Ni–B nanocatalyst for efficient hydrogen evolution reaction in wide pH range, Appl. Catal. B-Environ. 192 (2016) 123–133.

[31] Z. Fang, L. Peng, Y. Qian, X. Zhang, Y. Xie, J. J. Cha, G. Yu, Dual tuning of Ni–Co–A (A = P, Se, O) nanosheets by anion substitution and holey engineering for efficient hydrogen evolution, J. Am. Chem. Soc. 140 (2018) 5241–5247.

[32] X. Ren, D. Wu, R. Ge, X. Sun, H. Ma, T. Yan, Y. Zhang, B. Du, Q. Wei, L. Chen, Self-supported $CoMoS_4$ nanosheet array as an efficient catalyst for hydrogen evolution reaction at neutral pH, Nano Res. 11 (2018) 2024–2033.

[33] C. Pi, C. Huang, Y. Yang, H. Song, X. Zhang, Y. Zheng, B. Gao, J. Fu, P. K. Chu, K. Huo, *In situ* formation of N-doped carbon-coated porous MoP nanowires: a highly efficient electrocatalyst for hydrogen evolution reaction in a wide pH range, Appl. Catal. B-Environ. 263 (2020) 118358.

[34] J. Zhang, T. Wang, P. Liu, Z. Liao, S. Liu, X. Zhuang, M. Chen, E. Zschech, X. Feng, Efficient hydrogen production on MoNi4 electrocatalysts with fast water dissociation kinetics, Nat. Commun. 8 (2017) 15437.

[35] M. Fang, W. Gao, G. Dong, Z. Xia, S. Yip, Y. Qin, Y. Qu, J. C. Ho, Hierarchical NiMo-based 3D electrocatalysts for highly-efficient hydrogen evolution in alkaline conditions, Nano Energy 27 (2016) 247–254.

[36] Z. Dong, F. Lin, Y. Yao, L. Jiao, Crystalline $Ni(OH)_2$/amorphous $NiMoO_x$ mixed-catalyst with Pt-like performance for hydrogen production, Adv. Energy. Mater. 9 (2019) 1902703.

[37] S. Deng, X. Liu, T. Huang, T. Zhao, Y. Lu, J. Cheng, T. Shen, J. Liang, D. Wang, $MoO_2$ modulated electrocatalytic properties of Ni: investigate from hydrogen oxidation reaction to hydrogen evolution reaction, Electrochim. Acta 324 (2019) 134892.

[38] F. Wang, J. Chen, X. Qi, H. Yang, H. Jiang, Y. Deng, T. Liang, Increased nucleation sites in nickel foam for the synthesis of MoP@$Ni_3P$/NF nanosheets for bifunctional water splitting, Appl. Surf. Sci. 481 (2019) 1403–1411.

[39] Y. Zhou, C. Sun, X. Yang, G. Zou, H. Wu, S. Xi, Flame-like $Ni(OH)_2$ strongly promotes the dissociation of water and can be used to produce an excellent hybrid electrocatalyst for the hydrogen evolution reaction in alkaline media, Electrochem. Commun. 91 (2018) 66–70.

[40] M. A. R. Anjum, H. Y. Jeong, M. H. Lee. H. S. Shin, J. S. Lee, Efficient hydrogen evolution reaction catalysis in alkaline media by all-in-one $MoS_2$ with multifunctional active sites, Adv. Mater. 30 (2018) 1707105.

[41] W. Gao, W. Gou, X. Zhou, J. C. Ho, Y. Ma, Y. Qu, Amine-modulated/engineered interfaces of NiMo electrocatalysts for improved hydrogen evolution reaction in alkaline solutions, ACS Appl. Mater. Interfaces 10 (2018) 1728–1733.

[42] D. Huang, S. Li, Y. Luo, L. Liao, J. Ye, H. Chen, Self-templated construction of 1D NiMo nanowires *via* a Li electrochemical tuning method for the hydrogen evolution reaction, Nanoscale 11 (2019) 19429–19436.

[43] B. Zhang, J. Liu, J. Wang, Y. Ruan, X. Ji, K. Xu, C. Chen, H. Wan, L. Miao, J. Jiang, Interface engineering: The $Ni(OH)_2/MoS_2$ heterostructure for highly efficient alkaline hydrogen evolution, Nano Energy 37 (2017) 74–80.